EVALUATING SOIL NUTRITION STATUS WITH REMOTE SENSING DERIVED LAND PRODUCTIVITY

Meng Jihua, You Xingzhi, Chen Zhiqiang

Key Laboratory of Digital Earth
Institute of Remote Sensing and Digital Earth, Chinese Academy of Sciences
Beijing, China

ABSTRACT

Available nitrogen is the amount of this nutrient available to plants in the soil and the amount of nitrogen provided by fertilizers. Compared to total nitrogen, nitrogen availability is a more useful tool for determining how much fertilizer you need and when to apply it. Determining the level of nitrogen available in field soil is also a useful method to increase the efficiency of fertilizer. Most soil properties are time-consuming and costly to measure, and also change over time. Fast and accurate prediction of soil properties is a necessary to overcome the lack of measured soil property information. Satellite imagery provides contiguous spatial coverage of a field and can be used as a surrogate to measure soil attributes. In the past three decades, considerable progress has been made which prove the capacity and potential of remote sensing in soil science. The spectral characteristics of a number of nutrition content in soil have been studied and huge number of field nutrition mapping were implemented successfully.

Yet there still three major obstacles that prevent the wide application of remote sensing derived soil nutrition status map in precision farming, they are: 1) common remote sensing means cannot detect the entire soil body ("pedon") that extends from the surface to the parent material, not mention that the thin, upper layer sensed by optical sensors may easily be affected by many factors such as dust, rust, crop residue, plowing and particle size distribution; 2) in most studies that mapping soil nutrition status based on its spectral characteristics, high spectral resolution data are required, yet ever since the failure of EO-1 Hyperion in 2009, there has been a period of more than 4 years that has no satellite-mounted hyper-spectral images at the resolution higher than 30 m. The acquisition of hyper-spectral satellite image cannot be guaranteed. 3) crop coverage in crop growing season make it difficult to obtain soil radiometric property directly, the short period of soil explosion between crop seasons make it difficult to obtain satisfactory satellite images.

To deal with these three obstacles in mapping field soil nutrition status with satellite images, a new method was put forward and tested in mapping available nitrogen content. The basic concept of the method put forward by this research is that soil nutrition deficiency is the primary limitation on crop yield when other conditions are favorable (water, temperature and radiation). Firstly we map the crop yield of three major crops (wheat, soybean and maize) in last 4 years with a light use efficiency (LUE) model –CASA, which can integrate remote sensing indicators and meteorological data to describe crop growth. Secondly, yields of

different crops (wheat, soybean and maize) were normalized to make them comparable, a value (normalized yield index, NYI) between 0 and 1 were assigned to each pixel based on its place in the yield range of the crop type. Thirdly, the maximum NYI in the last 4 years was calculated for each pixel to represent the NYI in favorable crop growing conditions. At last the relationship between maximum NYI and observed soil available nitrogen content was identified through regression analysis, and then a map of field soil available nitrogen were produced.

In this study, taking HJ-1 CCD image as major data source and a farm in Northeast China as study area, the method proposed by the author was tested. The technical procedure, application and validation of this method were introduced in detail. After explore the potential of mapping field nutrition status with remote sensing derived crop yield, this paper provides some ideas on how to propel this technology forward to enable its widespread adoption in precision farming.

Keywords: Soil nutrition status; Available nitrogen concentration; Remote sensing; Crop yield

INTRODUCTION

Available nitrogen is the amount of this nutrient available to plants in the soil and the amount of nitrogen provided by fertilizers. Field tillage pattern and environmental conditions such as rainfall and temperature have a direct impact on the quantity of available nitrogen in the soil. The availability of nitrogen is often used to calculate the cost-to-benefit ratio of using fertilizer in a given area. Compared to total nitrogen, nitrogen availability is a more useful tool for determining how much fertilizer you need and when to apply it. Determining the level of nitrogen available in field soil is also a useful method to increase the efficiency of fertilizer. Using the level of nitrogen availability as a guide, one can accurately determine when to fertilize the crops.

Most soil properties (including soil available nitrogen) are time-consuming and costly to measure, and also change over time. Fast and accurate prediction of soil properties is a necessary to overcome the lack of measured soil property information.

In today's world of advanced technology various techniques are being used to study field parameters and gathering data for agricultural benefits. Remote sensing, for one, has a proven ability to provide spatial and temporal measurements of crop and field properties (Meng et al. 2013). In the past three decades, considerable progress has been made in such predictions following the development of remote technology. At this time, remote sensing appears to be an important and promising milestone in soil science (Ben-Dor et al. 2009). For the emerging discipline of precision agriculture, the remtoe sensing technology can assess fields before, during, and after the growing season, and thus provide farmers with a spatially explicit quantitative overview of the soil properties and phenomena in question.

In the last decade remote sensing has been proved useful to support precision farming by guiding field management as sowing, irrigation and fertilization. Yet the application of remote sensing to precision management of crops has suffered

from the cost and data availability constraints that restrict the wider application of satellite images (Zhang et al. 2002). As the performance of radiation sensors has improved, satellite and airborne receivers have provided increasingly detailed information on the reflected spectra, while fast digital processing of their output data, coupled with data fusion techniques, have led to a variety of powerful application (Sidney 2002).

Yet still there are several limitations that hinder the widely application of remote sensing in optimizing field fertilization:

(1) For all of these applications, single or even multi-band remote sensing means is rather limited and problematic when striving for quantitatively accurate information. For that purpose, high spectral resolution data are required. Based on comprehensive studies over the past decade that showed the VIS (400–700 nm), NIR (700–1100 nm), and SWIR (1100–2500 nm) spectral regions to serve as a powerful tools for recognizing soils qualitatively and quantitatively (Ben-Dor and Banin,1995a; Malley et al., 2004; Viscarra-Rossel et al., 2006). Only a few studies have successfully applied quantitative techniques to soil using low spectral and spatial resolution data (Ben-Dor and Banin, 1995c); ever since the failure of EO-1 Hyperion in 2009, there has been a period of more than 4 years that has no satellite-mounted hyper-spectral images at the resolution higher than 30 m. Pre-processing and converting the hyperspectral raw data into reflectance is a complicated process that requires experience, knowledge, and specific infrastructures not available to many users, whereas quantitative spectral models require good quality data (Ben-Dor et al. 2009). It requires expensive sensors, air hours, professional staff time and a sophisticated infrastructure that cannot be regularly used. Difficult and complex work in statistics and modeling is necessary. Beside that, the small coverage of hyper-spectral sensors also limited its application in wide area.

(2) Apparently, most of the optical remote sensing means cannot detect the entire soil body (“pedon”) that extends from the surface to the parent material. Moreover, the thin, upper layer that is eventually sensed by optical sensors may be affected by many factors such as dust, rust, plowing, particle size distribution, vegetation coverage, litter, and physical and biogenic crusts. Thus, optical remote sensing of soils from far distances becomes a significant challenge. The major limitation is that the entire soil profile, which is the ultimate parameter for soil classification, cannot be viewed because the radiation of the sun actually interacts with only the upper 50 mm of the soil surface (Ben-Dor et al., 1999).

(3) In addition, it should be remembered that the soil surface is not always flat, smooth, or homogenous and therefore sample preparation (as is done in the lab) is almost impossible. This leads to problems such as variations in particle size, adjacency, Bidirectional Reflectance Distribution Function (BRDF) effects, which may further reduce the accuracy (Ben-Dor et al. 2009). Partial or complete coverage of weeds, growing crops and crop residue will further reduce the signal of soil in the spectral reflectance information.

These limitations serve as a barrier that impedes potential end-users, inhibiting researchers from trying this technique for their needs of mapping soil nutrition parameters. To deal with these limitations and, this paper tests the concept of evaluating soil available nutrition parameters with indirect remote snesing

indicators---farmland productivity for avalible nitrogen in this case. This may be helpful to promote the application of satellite remote sensing in mapping soil available nutrition content---once it is proved that those nutrition parameters (namely available N, P, K) which are hard to map with their indistinctive spectral charsacteristics can be evaulated with other remote sensing derived indicator.

MATERIALS AND METHODS

Although it has long been proposed that assessing the plants' status during the growing season can provide indirect information about the soil situated underneath its canopy (Palacios-Orueta et al., 1999), its potential has never been fully utilized. Unlike commonly researches focus on the spectral characteristic of soil properties, this research will used yield as indirect indicator to evaluate soil nutrition status.

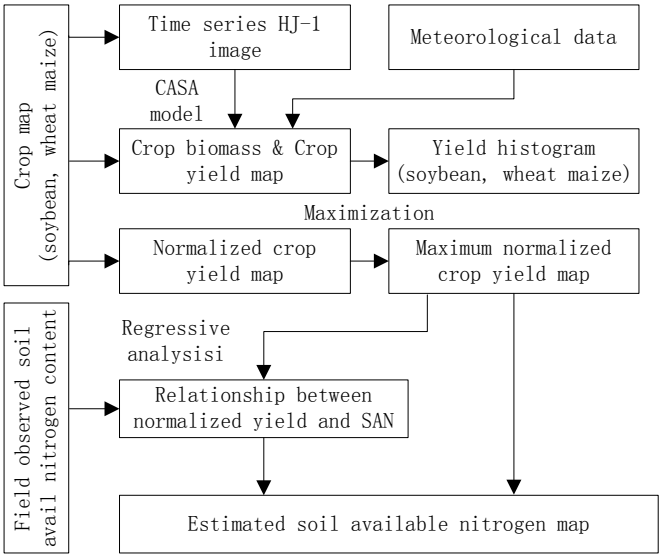

Figure 1 Technical process of the soil available nitrogen estimation

One of the primary principles of soil property prediction is “when predicting a variable, there should be a physical basis for the predictors” (Minasny and Hartemink 2011). The basic concept of the method put forward by this research is that soil nutrition deficiency is the primary limitation on crop yield when other conditions are favorable (water, temperature and radiation). Firstly we map the crop yield of three major crops (wheat, soybean and maize) in last 4 years with a light use efficiency (LUE) model –CASA, which can integrate remote sensing indicators and meteorological data to describe crop growth. Secondly, yields of different crops (wheat, soybean and maize) were normalized to make them comparable, a value (normalized yield index, NYI) between 0 and 1 were assigned to each pixel based on its place in the yield range of the crop type. Thirdly, the maximum NYI in the last 4 years was calculated for each pixel to represent the NYI in favorable crop growing conditions. At last the relationship between maximum NYI and observed soil available nitrogen content was identified

through regression analysis, and then a map of field soil available nitrogen were produced.

I. Experimental set up and field campaign

The study area, Hongxing Farm, locates in the north of Heilongjiang province, Northeast China (48°48′N, 125°31′ E). This place lies within the Mid-Temperate Zone characterized by average annual precipitation of 555mm and average annual accumulative temperature (higher than 10 celsius degree) of 2250 celsius degree. The major crops are soybean, spring corn and spring wheat. Corn and soybean account for more than 90% of total crops in the area.The growing season of study area is from beginning of May to end of October. The acreage of the farm is 76,000 acres, with an average field size of 1,500 acres.

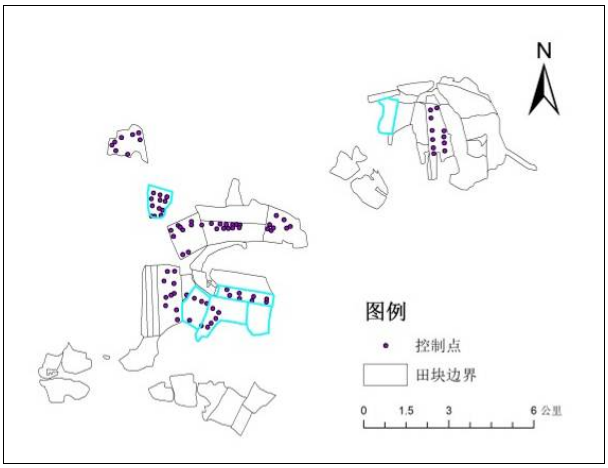

Figure 2 Study area (Shuangshan Farm) and experimental sites

The field campaigns were carried out between 25th, Apr. and 1st, May (before the start of the crop growing season) in 2013. Totally 89 sites were selected in 2011 (Fig. 1). Each site can represent a relative homogeneous area of 30m×30m. All the sites are located in cron and soybean planting plots. When more than one sites are located in one plot, the average distance between neighboring sites was controlled at 300m. Four soil samples were collected in each site, with a total sampled soil weight of 24g (6g for each sample) for each site. Soil sampling was performed at soil depths of 0-10 and 10–20 cm, the soil sampled at these two depths was mixed to test the available nitrogen content of the site. The SAN content were measured by Kjeldahl method. The GPS coordinates was recorded at the center of each site.

II. HJ-1 data and its pre-processing

The HJ-1 constellation system, which belongs to Environment and Disaster Observing Satellite System of China, consists of two small optical remote sensing satellites (HJ-1A and HJ-1B) and a microwave satellite (HJ-1C satellite) (Wang 2012). The satellites were planned for use in monitoring environment and natural disasters. HJ-1A/B satellites were launched successfully in September 2008. The onboard imaging systems and infrared cameras provide a global scan every two

days. HJ-1 satellites combine two identical CCD cameras that observe a broad coverage of 360 km with a high spatial resolution of 30 m. The CCD cameras have four visible and near-infrared bands, which include B1 (0.430.52 mm), B2 (0.520.60 mm), B3 (0.630.69 mm), and B4 (0.760.90 mm).

Cloud-free HJ-1A/B CCD images covering the Hongxing between 15th, April and 10th, October in 2010-2013 were gathered from China Centre for Resources Satellite Data and Application (CRESDA). The data used are listed in table 1:

Table 1. Dates of HJ -1 CCD images used in this study.

DATE (DD/MM/YY)		
2010	2011	2012
26/07/2011	**26/07/2011**	**26/07/201**
11/08/2011	**11/08/2011**	**11/08/201**
26/08/2011	**26/08/2011**	**26/08/201**
10/09/2011	**10/09/2011**	**10/09/201**
05/08/2011	**05/08/2011**	**05/08/201**
16/08/2011	**16/08/2011**	**16/08/201**
29/08/2011	**29/08/2011**	**29/08/201**
01/09/2011	**01/09/2011**	**01/09/201**
10/09/2011	**10/09/2011**	**10/09/201**

The HJ-1 images were released on the website in the form of multi-bands DN (digital number) grid. We converted the digital numbers of images to at-sensor reflectance and normalize it to a uniform solar zenith angle (thermal band not included). The equation to calculate reflectance is:

$$\rho=DN/ C_0^* + M_0^*, \quad \rho^*=\rho/\cos(\theta s) \tag{1}$$

where ρ is spectral reflectance at sensor, DN is the digital value of each pixel, C_0^* and M_0^* are the gain and bias of conversion, ρ* is the normalized reflectance, θs is the solar zenith angle. The gain and bias in the conversion are provided by CRESDA (http://www.creada.com). Then the FLAASH model in the ENVI software was used during the atmospheric correction procedure. Accurate geometric correction was done with ground control points derived from 1:50000 topographic maps. A final geo-correction error of less than 0.5 pixels was achieved.

III. Crop biological yield mapping

Crop yield (Y) was computed by (1), with the above ground biomass ($BIOMASS_{AGB}$) and harvest index (HI). While crop biomass is estimated with remote sensing data, HI is required from field observation data analysis.

$$Y = BIOMASS_{AGB} \times HI \tag{2}$$

The accumulation of aboveground biomass is proportional to accumulated APAR (Absorbed Photosynthetically Active Radiation) according to the Monteith model (Monteith, 1972):

$$AGB = \sum (APAR(t) \times \varepsilon(t)) \tag{3}$$

where AGB is the accumulated aboveground dry biomass in period t, ε (g MJ-1) represents the light use efficiency (LUE) and t describes the period over which accumulation takes place. APAR can be approximated directly from photosynthetically active radiation (PAR) and the fraction of PAR absorbed by photosynthetic tissues (FPAR). PAR (0.4-0.7 μm) is part of the short wave solar radiation (0.3-3.0μm) which is absorbed by chlorophyll for photosynthesis in plants, and PAR is thus a fraction (0.48 in this study) of incoming solar radiation. PAR could be estimated from the simple ratio (SR) by linear functions, and here FPAR was calculated as a linear function of SR, following Sellers et al. (1996):

$$FPAR = \frac{(SR - SR_{\min}) \times (FPAR_{\max} - FPAR_{\min})}{SR_{\max} - SR_{\min}} + FPAR_{\min} \tag{4}$$

$$SR = \frac{NIR}{RED} = \frac{1 + NDVI}{1 - NDVI} \tag{5}$$

where NIR and RED are the near-infrared and red reflectance, respectively. SR is the value of the simple ratio at a given pixel, SRmin and SRmax are related to the vegetation variety (here they correspond to the 5th and 95th percentile of SR for all cropland). FPARmin and FPARmax are defined as 0.01 and 0.95, respectively.

LUE is calculated as the product of an optimal LUE (ε*) and its temperature and water stressors

$$\varepsilon(t) = \varepsilon^* \times T_1(t) \times T_2(t) \times W(t) \tag{6}$$

where ε* is the typical maximum LUE for aboveground biomass when the environmental conditions are optimal. T1, T2, and W are scalars representing environmental stressors that reduce LUE under unfavorable conditions (Field et al., 1995). T1 represents a physiological reduction of LUE at both very low and very high temperatures (higher or lower than an optimal temperature (Topt (℃)), defined as mean air temperature during the month of maximum NDVI development). T2 reduces LUE as temperatures deviate from 20℃, representing constraints beyond physiological compensation at extreme temperatures. W is a water condition down-regulator. T1 and T2, are calculated with the following formulas (Field et al., 1995).

$$T_1 = -0.0005(T_{opt} - 20)^2 + 1 \tag{7}$$

$$T_2 = \frac{1}{1 + \exp\{0.2(T_{opt} - 10 - T_{mon})\}} \times \frac{1}{1 + \exp\{0.3(-T_{opt} - 10 + T_{mon})\}} \tag{8}$$

where Tmon (℃) is the mean monthly air temperature.

Time series of ET (evpotranspiration) from ETWatch (Xiong et al., 2010) was used in estimating water stress in biomass production.

VI. Yield Normalization

The major crops in the study area are maize, wheat and bean. To make the yield of different crops comparable, the yield of each crop (namely maize, wheat and bean) was normalized to a value between 0 and 1. In this process, firstly we use a normal function to fit the PDF (probability density function) of each crop; then the average yield of the crop and its standard devaition were derived; at last we define a minium and a maximum thresholds to normalize crop yieds. The equation for yield normalization is listed below:

$$yield_{nor}=(yield-yield_{min})/(yield_{max}-yield_{min}) \quad (9)$$

where $yield_{nor}$ is the normalized crop yield, yield is pixel value on crop yield map, $yield_{max}$and $yield_{min}$ are the predefined maximum and minimum yield thresholds, which are computed as the following formulas:

$$yield_{max}=yield_{ave}+2*\delta \quad (10)$$
$$yield_{min}= yield_{ave}-2*\delta \quad (11)$$

where $yield_{ave}$ is the average crop yield for each crop andδ is the standard devaition of the yield.

After crop yield normalization, the maximum normalized yield index (NYI) were computed for each pixel along the time series 2010-2012. We assume this NYI map can resprenent the NYI at favorable growing conditions (when SAN is the dominant limitation for crop yield).

V. Regression analysis

In this paper, the focus is on exploring the feasibility of estimation SAN with multi-year remote sensing derived crop yield map. To determine whether these remote sensed indicators are sensitive to SAN, correlation coefficients were computed with the following formula:

$$r = \frac{\sum_{i=1}^{n}(Ri - Rave)(SANi - SANave)}{\sqrt{\sum_{i=1}^{n}(Ri - Rave)^2}\sqrt{\sum_{i=1}^{n}(SANi - SANave)^2}} \quad (2)$$

Where *Ri* is the remote sensing derived indicators in the image pixel that spatially match the *i*th field observations, *Rave* is the average of sensing derived indicators, *SANi* is the observed SAN of site *i* and SAN*ave* is their average.

RESULTS AND DISCUSSION

I. Crop yield map

The remote sensing derived crop yield of 2010-2012 were listed in figure 3:

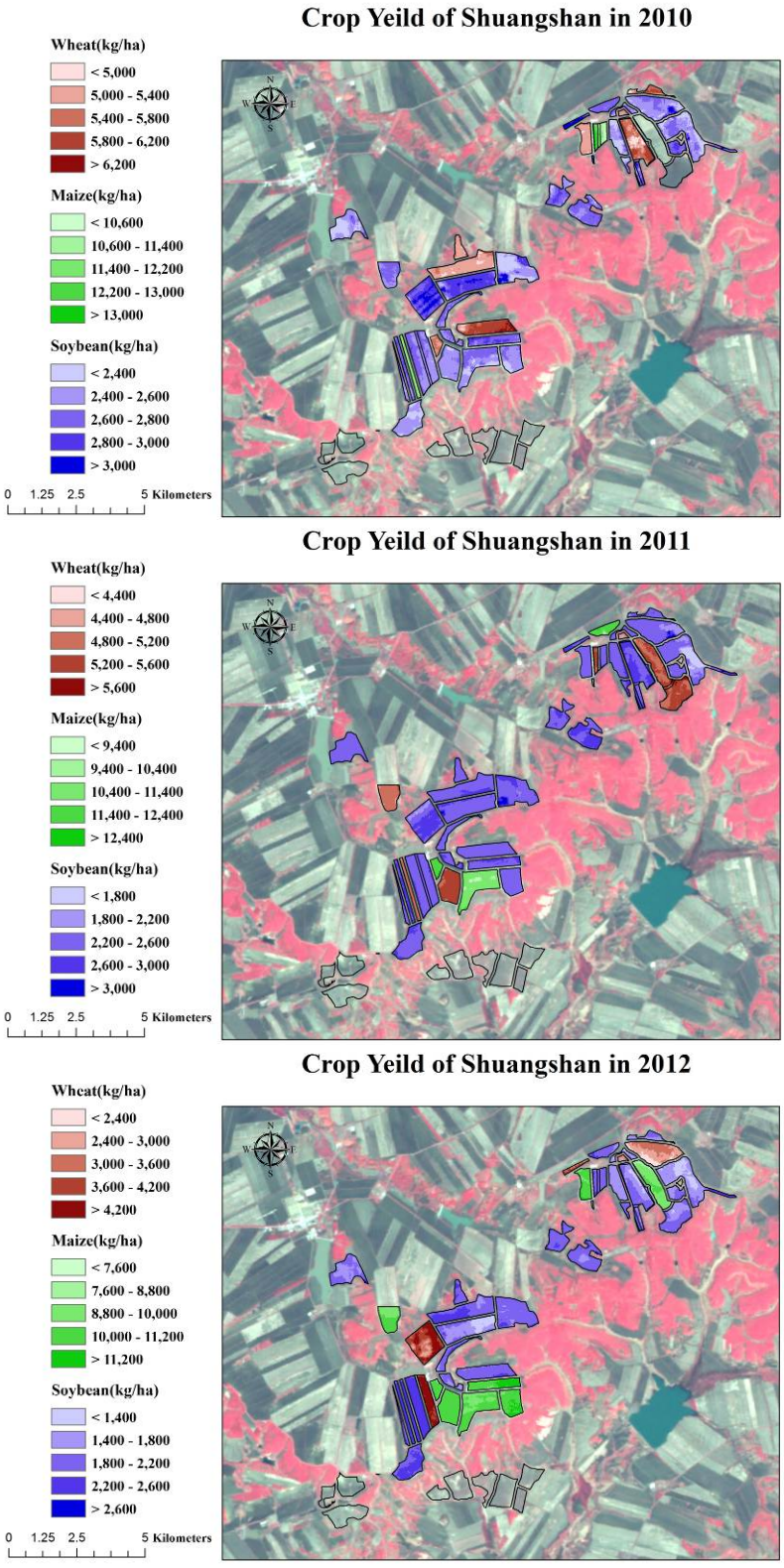

Figure 3. Yield for major crops of Shuangshan (2010-2012)

Brown, green and cyan colors are used to presnent the yield of wheat, maize and soybean. The yield for wheat is between 2400-6200 kg/ha, and that for soybean and maize are 1400-3000 kg/ha and 7600-13000 kg/ha. Generally speaking, the yield of 2010 is higher than that in 2011 and 2012, this is because a

more favorable meteorological consition (temperature and precipation) was witnessed in 2010.

II. Yield normalization and maximum NYI map

The PDF for yield normalization for wheat, maize and soybean are listed in figure 4:

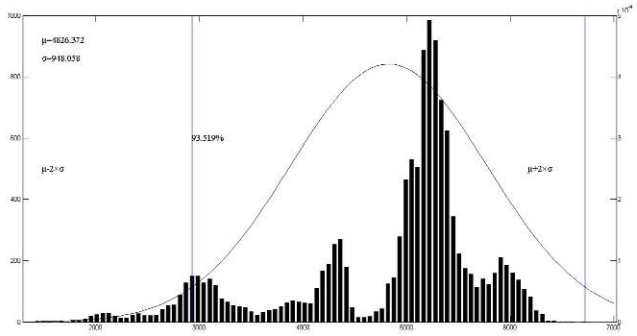

(a) wheat

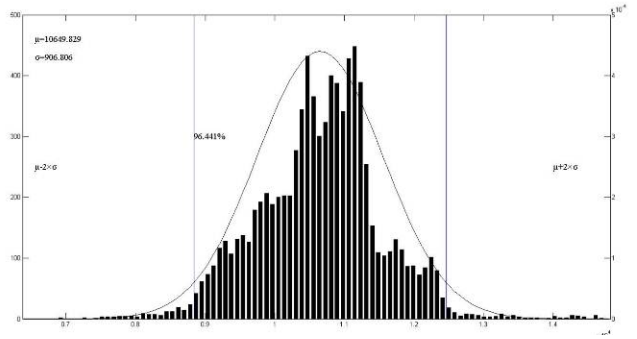

(b) maize

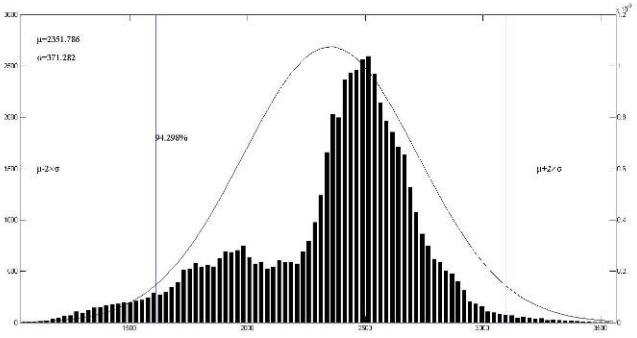

(c) soybean

Figure 4. The PDF for yield normalization for wheat, maize and soybean

After normalization, maximum NYI was cromputed (fiure 5):

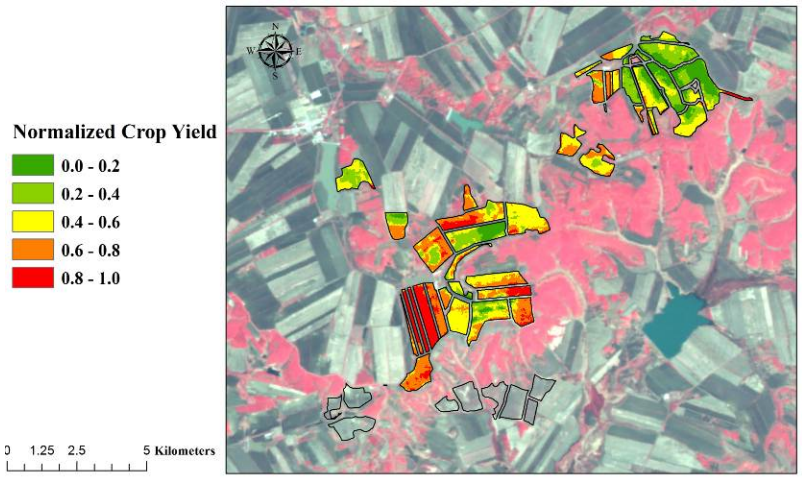

Figure 5. The maximum NYI map of Shuangshan

III. SAN estimation model and SAN map

Based on spatial matching, the relationshop between NYI and observed SAN was analyzed. Figure 6 quantitative relationship between them.

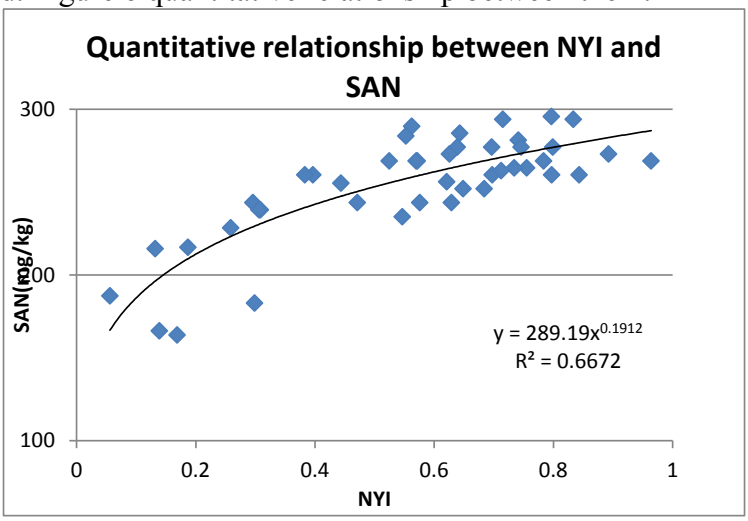

Figure 6. Quantitative relationship between NYI and SAN

Based on the model derived from Figure 6, the SAN map of Shuangshan were derived (figure 7):

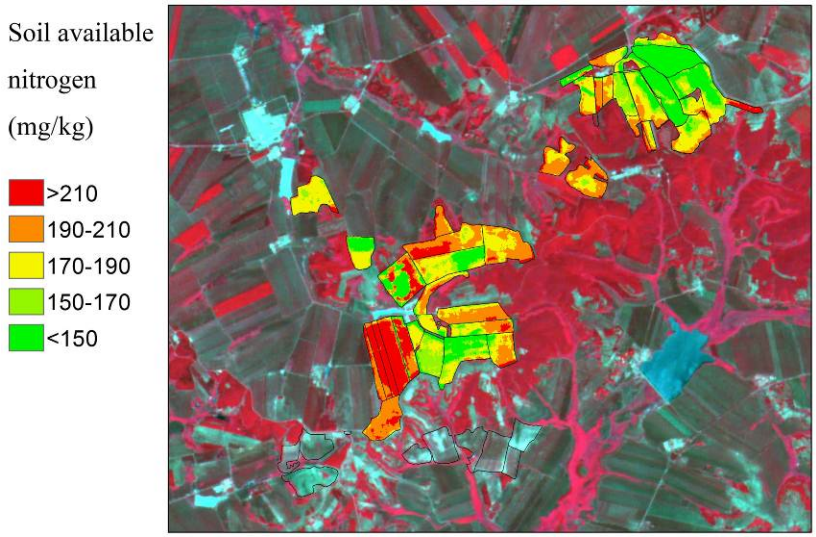

Figure 7. Estimated SAN map of Shuangshan

According to the SAN map derived in this study, the SAN in Shuanshan farm varied from 120 to 260 mg/kg. Fields on the west tends to have a higher SAN (above 210) than fields on the east (lower than 150). The SAN not only varies between fields, the in-fields variation of SAN could also be as high as 100 mg/kg.

DISCUSSION AND CONCLUSION

The method and analysis presented in this paper is intended to respond to the increasing needs in optimizing field management with earth observation technology, namely fertilization management specifically. The discussion of this paper will focus on the advantage, disadvantage and uncertainties of the study, as well as proposing future research focus in this field.

Advantage: The proposed approach exploits inherent relationship between crop yield and field soil nutrition status, it can provide new information on soil that cannot be extracted by field work using traditional soil sampling or point spectrometry measurements. Compare to common method that estimating soil nutrition status with satellite image from its spectral characteriscs, the method put forward in this study can map soil status at a certain soil depth and no hyper-spectral data is required.

Limitation: Along with these advantages, this approach also has inherent limitations. The method only works when SAN is the dominant limiting factor of crop yield. But in real crop growing conditions, factors like drought, topographty and other meteorological conditions all have influence on crop yield. The effect of SAN on crop yield is hard to be distinguished from that of other factors. Although the computation of maximum NYI may alleviate the influence of other factor, the influence of continuous unfavorable growing conditions still can not be removed.

Uncertainties: Crop yield estimation is implemented in this research to estimate SAN. The performance of yield estimation model is not analyzed in this paper, yet the inaccuracy in yield mapping will certainly induce uncertainty in the result.

ACKNOWLEDGEMENTS

This work was funded by the National Natural Science Foundation of China (41171331, 41010118). Additionally, we thank the CRESDA for providing the HJ-1 data.

REFERENCES

E. Ben-Dor, S. Chabrillat, J.A.M. Demattê, G.R. Taylor, J. Hill, M.L. Whiting, S. Sommer. Using Imaging Spectroscopy to study soil properties. Remote Sensing of Environment 113 (2009) S38-S55

Ben-Dor, E., & Banin, A. (1995a). Near infrared analysis (NIRA) as a simultaneously method to evaluate spectral featureless constituents in soils. Soil Science, 159, 259−269.

Malley, D. F., Martin, P., & Ben-Dor, E. (2004). Application in analysis of soils. Chapter 26. In R. Craig, R. Windham, & J. Workman (Eds.), Near infrared spectroscopy in agriculture A three Societies Monograph (ASA, SSSA, CSSA), vol. 44 (pp. 729–784).

Viscarra-Rossel, R. A., Walvoort, D. J. J., Mcbratney, A. B., Janik, L. J., & Skjemstad, J. O. (2006). Visible, near infrared, mid infrared or combined diffuse reflectance spectroscopy for simultaneous assessment of various soil properties. Geoderma, 131, 59−75.

Ben-Dor, E., & Banin, A. (1995c). Quantitative analysis of convolved TM spectra of soils in the visible, near infrared and short-wave infrared spectral regions (0.4–2.5 mm). International Journal of Remote Sensing, 18, 3509−3528.

Ben-Dor, E., Irons, J. A., & Epema, A. (1999). Soil Spectroscopy. In A. Rencz (Ed.), Manual of Remote Sensing (pp. 111−188). Third edition. NewYork: J. Wiley & Sons, Inc.

Budiman Minasny, Alfred E. Hartemink. Predicting soil properties in the tropics. Earth-Science Reviews 106 (2011) 52–62

Meng, J., Du, X., and Wu, B. Generation of high spatial and temporal resolution NDVI and its application in crop biomass estimation, International Journal of Digital Earth, 2013, 6 (3): 203-218

Monteith, J.L., 1972. Solar radiation and productivity in tropical ecosystems. J. Appl. Ecol. 9, 747–766.

Field, C.B., Randerson, J., and Malmstrom, C.M., 1995. Global net primary production: combining ecology and remote sensing. Remote Sensing of Environment, 51, 74-88.

Xiong, J., Wu, B., Yan, N., Zeng, Y., and Liu, S., 2010. Estimation and validation of land surface evaporation using remote sensing in North China. IEEE Journal of Selected Topics in Applied Earth Observations and Remote Sensing, Conference special issue. 3(3), 337-344